Carbohydrate Polymers 119 (2015) 173–181

Contents lists available at ScienceDirect

Carbohydrate Polymers

journal homepage: www.elsevier.com/locate/carbpol

Microencapsulation of alginate-immobilized bagasse with *Lactobacillus rhamnosus* NRRL 442: Enhancement of survivability and thermotolerance

Shahrulzaman Shaharuddin [a], Ida Idayu Muhamad [a,b,*]

[a] Department of Bioprocess Engineering, Faculty of Chemical Engineering, Universiti Teknologi Malaysia, 81310 UTM Skudai, Johor Bahru, Johor, Malaysia
[b] IJN-UTM Cardiovascular Engineering Centre, Universiti Teknologi Malaysia, 81310 UTM Skudai, Johor Bahru, Johor, Malaysia

ARTICLE INFO

Article history:
Received 25 August 2014
Received in revised form
20 November 2014
Accepted 24 November 2014
Available online 3 December 2014

Keywords:
Encapsulation
Immobilization
Alginate
Bagasse
Lactobacillus
Heat

ABSTRACT

The aim of this research was to enhance the survivability of *Lactobacillus rhamnosus* NRRL 442 against heat exposure via a combination of immobilization and microencapsulation processes using sugarcane bagasse (SB) and sodium alginate (NaA), respectively. The microcapsules were synthesized using different alginate concentration of 1, 2 and 3% and NaA:SB ratio of 1:0, 1:1 and 1:1.5. This beneficial step of probiotic immobilization before microencapsulation significantly enhanced microencapsulation efficiency and cell survivability after heat exposure of 90 °C for 30 s. Interestingly, the microcapsule of SB-immobilized probiotic could obtain protection from heat using microencapsulation of NaA concentration as low as 1%. SEM images illustrated the incorporation of immobilized *L. rhamnosus* within alginate matrices and its changes after heat exposure. FTIR spectra confirmed the change in functional bonding in the presence of sugarcane bagasse, probiotic and alginate. The results demonstrated a great potential in the synthesis of heat resistant microcapsules for probiotic.

1. Introduction

According to Food and Agriculture Organization (FAO) of the United Nations and the World Health Organization (WHO), probiotic means live microorganisms which provide health benefits to hosts when administrated in sufficient amounts (FAO/WHO, 2002). Health and growth benefits offered by probiotic make them a highly potential additive in the animal feed industry. Moreover, the prospect of probiotic as an alternative to antibiotics has been considered (Kosin & Rakshit, 2010). Lactic acid bacteria are one of the largest groups of probiotic and most of *Lactobacillus* sp. was regarded as animal probiotic. In this study, *Lactobacillus rhamnosus* was used as probiotic model due to its beneficial effects on ruminant animal.

Probiotics have been included in various products such as food (Anal & Singh, 2007) and feed (Gaggìa, Mattarelli, & Biavati, 2010). The main concern of this supplement is low viability of free probiotic in end products that could no longer provide the health benefits (Burgain, Gaiani, Linder, & Scher, 2011; De Vos, Faas, Spasojevic, Sikkema, 2010). In practice, probiotic animal feed involve with high thermal treatment during pelleting process. However, this has resulted in low viability of the final product due to heat-sensitive characteristic of probiotic that explained the importance of viability maintenance to deliver its benefit to host health or growth (Seo et al., 2010). This challenge created an opportunity for the development of thermal protection technique which may reduce the exposure effect of lethal temperature.

Cell immobilization on solid carrier can be defined as localization of intact cell via physical adsorption between the carrier and cell membrane (Kourkoutas, Bekatorou, Banat, Marchant, & Koutinas, 2004). This technique has been widely used in enhancing and maintaining viability of probiotic during product processing and storage. Many studies of probiotic immobilization on solid carriers have been performed previously using apple pieces (Corbo, Bevilacqua, Gallo, Speranza, & Sinigaglia, 2013), quince (Kourkoutas, Xolias, Kallis, Bezirtzoglou, & Kanellaki, 2005), wheat (Bosnea et al., 2009), cereal (Michida et al., 2006), bacterial cellulose (Jagannath, Raju, & Bawa, 2010), watermelon rind (Reddy, Reddy, Reddy, & Reddy, 2008) and pear (Kourkoutas, Bosnea, et al., 2006).

Microencapsulation technique promotes the concept of a physical barrier that offers better protection of probiotic and safe delivery

* Corresponding author at: Department of Bioprocess Engineering, Faculty of Chemical Engineering, Universiti Teknologi Malaysia, 81310 UTM Skudai, Johor Bahru, Johor, Malaysia. Tel.: +60 7 5535577.
E-mail addresses: sshahrulzaman@gmail.com (S. Shaharuddin), idayu@cheme.utm.my (I.I. Muhamad).

http://dx.doi.org/10.1016/j.carbpol.2014.11.045
0144-8617/

to target (Burgain et al., 2011). Characteristics of microcapsules include variation in size from a few microns to 1 mm, shape, thickness and strength of wall (Anal & Singh, 2007). Generally, the main objective in microencapsulation of probiotic is to enhance their survivability and maintain viability to the maximum log CFU, at least up to minimum concentration in delivering their beneficial effect to host (Anal & Singh, 2007; Rokka & Rantamaki, 2010). Probiotic can resist adverse and stress conditions such as acidity, oxygen and gastric environment using encapsulatant wall (Borgogna, Bellich, Zorzin, Lapasin, & Cesaro, 2010; Burgain et al., 2011; Rokka & Rantamaki, 2010).

Immobilization and microencapsulation provide better protection of probiotic towards thermal exposure. Some delivery paths may necessitate passing through thermal exposure before reaching the targeted place. Various studies on thermal resistance using different types of immobilization medium were performed via technique of immobilization attachment (Kannoujia, Ali, & Nahar, 2009; Kourkoutas et al., 2005; Nagar, Mittal, Kumar, Kumar, & Gupta, 2012; Quan, Liu, Branford-White, Nie, & Zhu, 2014) and microencapsulation (Chen, Chen, & Kuo, 2007; Chitprasert, Sudsai, & Rodklongtan, 2012; Ding & Shah, 2009; Karakuş & Pekyardımcı, 2009; Mandal, Puniya, & Singh, 2006; Noriega, Velliou, Van Derlinden, Mertens, & Van Impe, 2013; Sabikhi, Babu, Thompkinson, & Kapila, 2010). Promising potential of thermotolerance via both techniques were demonstrated and its application could be used in other sectors such as animal feed processing.

The objective of this study was to increase the survivability of model probiotic, *L. rhamnosus* NRRL 442 against heat exposure via heat barrier microcapsule. Sugarcane bagasse (SB) was incorporated into the microcapsule as a filler. Sodium alginate (NaA) was used as encapsulant and calcium chloride as crosslinker. The incorporation may affect the physicochemical properties due to molecular interactions of encapsulant agent and filler. Alginate is a simple, non-toxic, biocompatible and low cost biomaterial (Krasaekoopt, Bhandari, & Deeth, 2003) while SB is cheap, renewable and an abundantly available worldwide biopolymer (Karnitz, Gurgel, & Gil, 2010; Mandal & Chakrabarty, 2011; Vercelheze et al., 2012). It consists of 2.7–2.8%, 9.8–10% and 0.3–0.5% of protein, crude fibre and fat, respectively (Shaharuddin, Muhamad, Seng, Zahan, & Khairuddin, 2014). *L. rhamnosus* is one of the well-documented probiotic that may provide health benefit to the ruminant animal (Gaggìa et al., 2010). Extrusion method was used for the production of novel cell-loaded alginate-SB composite microcapsule. The characteristics of microcapsules were analyzed for the encapsulation efficiency, particle size, morphology and FTIR spectra. The maximum microencapsulation condition was determined after the microcapsules were treated with heat and the cell viability and morphology were analyzed. All data were statistically analyzed using one-way ANOVA and Duncan's multiple range test (DMRT).

2. Materials and methods

2.1. Materials

Sodium alginate (Q-ReC), calcium chloride (Q-ReC), peptone water (Sigma–Aldrich), sodium citrate (Q-ReC), MRS broth (Merck), MRS agar (Merck) and potassium bromide (Merck) were of analytical grade. All chemicals were used without further purification. *L. rhamnosus* NRRL 442 used as probiotic model was received from Agricultural Research Service (ARS, USA). Fresh SB was collected from local supplier in Johor Bahru, Johor, Malaysia. Three replications were done for each sample. Fresh SB was ground and sieved using 75 μm mesh. Then SB was dried using hot air oven at 40 °C for 48 h and kept in freezer (−20 °C).

2.2. Microencapsulation of immobilized L. rhamnosus

The microencapsulation of *L. rhamnosus* NRRL 442 began with the immobilization of the probiotic on SB followed by mixing with alginate. Then the Lr–SB–NaA solution was extruded and ended with droplet gelation via ionic crosslinking. Microencapsulation was performed by slight modification of the procedure described by Chen et al. (2007). The immobilized probiotic was prepared with stock culture of *L. rhamnosus* NRRL 442 inoculated into sterile culture medium, agitated in orbital shaker at 200 rpm with incubator at 37 °C for 16–18 h. A probiotic cell suspension was prepared by centrifuging the culture medium at 10,000 rpm for 3 min (Seng, Muhamad, Tin, Razali, Pae, & Shaharudin, 2012). The cells were washed and resuspended in 0.1% peptone solution. The probiotic was microencapsulated via extrusion technique. Coating material were prepared using 1, 2 or 3% (w/v) of sodium alginate and autoclaved (121 °C, 15 min). The coating material was mixed with immobilized probiotic-SB at different dry weight ratio of 1:0, 1:1 and 1:1.5 (w/w). The homogenized mixture of immobilized probiotic-SB and coating solution was extruded through modified syringe into sterile 0.1 M $CaCl_2$. The formed microcapsules were allowed to stand for 1 h for solidification, then rinsed and subsequently kept in sterile 0.1% peptone solution at 4 °C for further analysis.

2.3. Microencapsulation efficiency

In order to determine the microencapsulation efficiency of *L. rhamnosus*, 1 g of microcapsules was dissolved by placing them in 50 mL sodium citrate solution (10 g/L) until disintegration using stirrer. The cell viability was determined by colony forming units (CFU/g) counting via a pour-plate method using MRS agar and then incubating at 37 °C for 48 h. Microencapsulation efficiency (ME) was calculated using Eq. (1):

$$\mathrm{ME}\,(\%) = \frac{N}{N_0} \times 100 \quad (1)$$

where N is the number of microencapsulated cells released from the microcapsules (log CFU/g microcapsule) and N_0 is the number of free cells added to the polymer mixture during the production of the microcapsules (log CFU/g).

2.4. Microcapsule size

Diameter of ten wet beads was evaluated using calliper (Mitutoyo, Japan) and the average diameter were measured and recorded. The measurement was replicated three times.

2.5. Morphology analysis via SEM

The morphological study was observed by Scanning Electron Microscope (SEM, Phenom G2 Pro). The sample was dried and fixed to double sided conductive tape on top of SEM stub. SEM was operated at 15 kV with 1000× magnification.

2.6. Fourier transform-infrared spectroscopy (FT-IR)

The sample was characterized using FTIR spectroscopy to study the chemical composition and bonding present. Samples were mixed and pulverized with a mortar and pestle with potassium bromide (1:100) and compressed into tablets. The FT-IR analysis was carried out using a FT-IR Spectrometer (Spectrum 2000 Explorer, Perkin-Elmer, Waltham, MA), with a resolution of 4 cm^{-1} in the range of 4000–400 cm^{-1}.

Table 1
Microencapsulation efficiency and yield of microcapsules synthesized under different condition.

NaA concentration (%)	NaA:SB ratio	Micoencapsulation efficiency (%)
1	1:0	86.70 ± 1.70^{ab}
	1:1.0	87.10 ± 0.85^{abc}
	1:1.5	89.30 ± 1.00^{c}
2	1:0	87.10 ± 0.85^{abc}
	1:1.0	89.35 ± 0.49^{c}
	1:1.5	89.35 ± 0.21^{c}
3	1:0	85.25 ± 0.92^{a}
	1:1.0	87.60 ± 1.13^{abc}
	1:1.5	88.35 ± 0.92^{bc}

Means with different superscripts (a–c) within a column were significantly different [$P < 0.05$, $n = 3$].

Table 2
Sizes of microcapsule.

NaA concentration (%)	NaA:SB ratio	Microcapsule diameter (μm)
1	1:0	292.80 ± 37.30^{a}
	1:1.0	373.20 ± 74.09^{b}
	1:1.5	486.20 ± 68.67^{cd}
2	1:0	340.70 ± 26.88^{ab}
	1:1.0	457.60 ± 77.20^{c}
	1:1.5	505.30 ± 70.56^{cde}
3	1:0	390.90 ± 52.43^{b}
	1:1.0	516.70 ± 45.78^{de}
	1:1.5	557.20 ± 55.01^{e}

Means with different superscripts (a–e) within a column were significantly different [$P < 0.05$, $n = 3$].

2.7. Heat exposure

Heat resistance test was performed by exposure of 1 g of free cell and immobilized/microencapsulated cell at 90 °C for 40 s and instant immersion in chilled water at room temperature within 3 min. The cell viability evaluation was performed as described previously in Section 2.3. The cell survivability was calculated according to Eq. (2):

$$\text{Cell survival}\,(\%) = \frac{N_h}{N_i} \times 100 \quad (2)$$

where N_i is the initial number of viable immobilized or/and microencapsulated cells before heat exposure (log CFU/g microcapsule); and N_h is the number of cells released from the SB/microcapsules after the heat exposure (log CFU/g microcapsule).

2.8. Statistical analysis

Nine combinations from full factorial design of two factors at three levels were derived and used for the experiment. All experiments were replicated three times. Statistical analysis was undertaken using one-way ANOVA. The data were presented as mean values ± standard deviation (SD). The statistical significance of the results was evaluated using Duncan's multiple range test (DMRT) at a significance level of $R = 0.05$.

3. Results and discussion

The resultant microcapsules in the form of microgels consist of immobilized *L. rhamnosus* NRRL 442 within SB matrices. The microcapsules were characterized to determine the optimum conditions of developed method and the performance of double protection towards probiotic after heat treatment process.

3.1. Microencapsulation efficiency

The microcapsules were analyzed via cell viability after the microencapsulation process and calculated as microencapsulation efficiency. It is crucial to obtain high efficiency of immobilization and encapsulation in order to maintain high viability as the resultant microcapsules will be subjected to heat treatment. Generally, there was high retainability or small loss of cell viability as recorded in Table 1. Microencapsulation process using NaA:SB ratio of (1:1.5) and (1:1) attained the highest efficiency of 89.35 ± 0.49 and 89.35 ± 0.21, respectively. No significant differences were observed in most conditions of preparing the microcapsules. This finding emphasized the benefit and importance of immobilization stage before microencapsulation. However, this is contradict to previous study that reported the incorporation of rice bran in microencapsulation of *Lactobacillus reuteri* KUB-AC5 provided less encapsulation efficiency compared to non-incorporation of the fibre (Chitprasert et al., 2012).

Interestingly, results showed incorporation of SB enhanced the retainability of probiotic after microencapsulation process in comparison to that without fibre incorporated. This indicated that immobilization of *L. rhamnosus* on SB before the microencapsulation stage had assisted in retention of cell viability hence further increased the efficiency. Incorporation of SB provides larger surface area for the attachment of probiotic before the microencapsulation. Moreover, dense structure of NaA–SB inside the microcapsule enables the immobilized probiotics to remain entrapped and encapsulant matrices only diffuse out water molecule. Eventhough inclusion of filler in microcapsule reduces the encapsulation efficiency, the strong adhesion of probiotic during immobilization alleviated this negative effect. The loss of cell viability was slightly affected by the extrusion during the microencapsulation process. In addition, the high efficiency was also due to non-toxicity of NaA as encapsulant agent.

3.2. Particle size

The size of microcapsule affects the homogeneity and dosage of additive in the pellet feed (Chitprasert et al., 2012). Smaller additive size may provide better distribution subsequently improving the homogeneity and dosage of the additive. In pelleting process, the adequate and recommended size range of feed additive is 50–500 μm (Chitprasert et al., 2012). Table 2 showed the microcapsule size synthesized from the nine different combinations of microencapsulation performed in this study. The microcapsules ranged in size from 292.80 to 557.20 μm. The microcapsule diameter increased when the concentration of NaA and ratio of NaA:SB increased. The average sizes of microcapsules with pre-immobilized probiotic were significantly increased in comparison to that without immobilization process. This was observed in each concentration of NaA used and was due to the presence of SB component in the formation of microcapsule. However, the increase in microcapsule diameter was not significant when the NaA:SB ratio was increased from 1:1 to 1:1.5. This could be attributed to the fast flowing of mixing solution during extrusion which limited the space of immobilized probiotic on SB during encapsulation. In addition, acceptable microcapsule diameter was also archived due to the size reduction of SB after autoclave process (Chitprasert et al., 2012).

3.3. Surface morphology

The experimental effects of alginate concentration, inclusion of SB ratio and heat on the microcapsules were illustrated in Fig. 1. Evaluation involved eight different conditions of microencapsulation; i.e. microcapsules prepared from NaA:SB (1:0), NaA:SB (1:1.5),

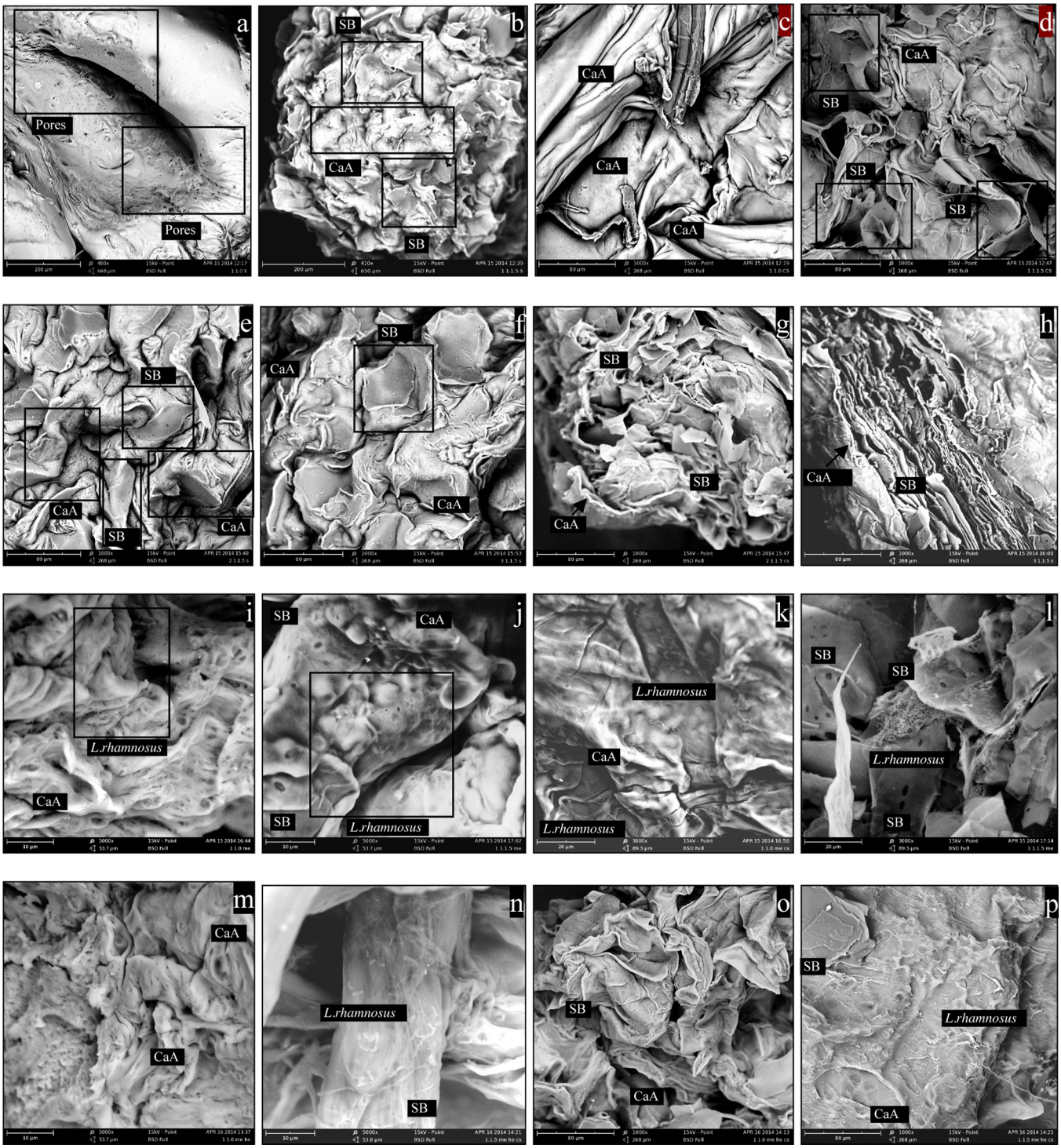

Fig. 1. SEM of NaA and NaA–SB microcapsule areas. Outer surface of NaA:SB (1:0) and NaA:SB (1:1.5) microcapsules (a and b, respectively). Inner surface of NaA:SB (1:0) and NaA:SB (1:1.5) microcapsules (c and d, respectively). Outer surface of NaA:SB (2:1.5) and NaA:SB (3:1.5) microcapsules (e and f, respectively). Inner surface of NaA:SB (2:1.5) and NaA:SB (3:1.5) microcapsules (g and h, respectively). Outer surface of NaA–SB (1:0) and NaA:SB (1:1.5) microcapsules loaded with *L. rhamnosus* NRRL 442 (i and j, respectively). Inner surface of NaA–SB (1:0) and NaA:SB (1:1.5) microcapsules loaded with *L. rhamnosus* NRRL 442 (k and l, respectively). Outer surface of heated NaA–SB (1:0) and NaA:SB (1:1.5) microcapsules loaded with *L. rhamnosus* NRRL 442 (m and n, respectively). Inner surface of heated NaA–SB (1:0) and NaA:SB (1:1.5) microcapsules loaded with *L. rhamnosus* NRRL 442 (o and p, respectively).

NaA:SB (2:1.5), NaA:SB (3:1.5), microcapsules loaded with *L. rhamnosus* NRRL 442 prepared from NaA:SB (1:0) and NaA:SB (1:1.5), heated microcapsules loaded with *L. rhamnosus* NRRL 442, prepared from NaA:SB (1:0) and NaA:SB (1:1.5). The alginate microcapsules without inclusion [NaA:SB (1:0)] of SB has approximately smooth outer surface with many porous regions (Fig. 1a). The smooth surface of alginate became crumpled, rugged and denser with the incorporation of SB [NaA:SB (1:1.5)] into the microcapsules (Fig. 1b). However, less porous regions were shown as the incorporated SB covered some regions of the microcapsule. Meanwhile, the inner surface of NaA:SB (1:0) and NaA:SB (1:1.5) microcapsules were similar to outer surfaces as their porous matrices were all over

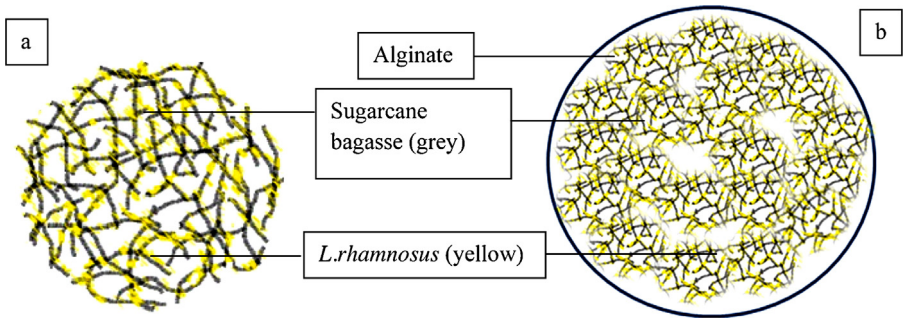

Fig. 2. Schematic diagram: (a) immobilized *L. rhamnosus* NRRL 442 on SB, (b) microcapsule of immobilized *L. rhamnosus* NRRL 442.

the surface (Fig. 1c and d). Less and smaller pores were observed at NaA:SB (1:1.5) microcapsules compared to NaA:SB (1:0) microcapsules. The surface of NaA:SB (1:1.5) was more compact to NaA:SB (1:0) and clearly showed the presence of congregated SB.

The outer surface morphology of increased concentration of NaA microcapsules from 2% to 3% were illustrated in Fig. 1e and f [ratio of NaA:SB (2:1.5) and NaA:SB (3:1.5)], respectively. Similar morphologies were obtained with crumpled and rugged surface between outer surfaces of both microcapsules. However, the surface became compact due to increasing of NaA amount in formulation. Less SB were observed on the surface of Fig. 1f as the NaA has covered most areas of the microcapsule. Fig. 1g and h showed the comparison of cross section of microcapsules prepared from NaA:SB (2:1.5) and NaA:SB (3:1.5), respectively. The inner surface of NaA:SB (3:1.5) has more layers of alginate and incorporated SB than NaA:SB (2:1.5) microcapsule. Compact structure of those layers was formed by increased NaA concentration. Similarly, images of both microcapsule surfaces showed more SB fractions in NaA:SB (2:1.5) microcapsule compared to NaA:SB (3:1.5) microcapsule. Again, the compactness places the incorporated SB in between each layer.

The presence of bulging probiotic *L. rhamnosus* can be observed in all samples after the inclusion (Fig. 1i–l). The probiotic was short, rod shaped and randomly distributed in all areas of surface. Encapsulated probiotic changed the surface of NaA–SB (1:0) microcapsule (Fig. 1i) into crumple and become uneven compared to its original structure (Fig. 1a). Similarly in NaA:SB (1:1.5) microcapsule, the short rod-shaped probiotic could be seen in almost all region of surface. This phenomenon relates to the immobilization process that contributed to high attachment of probiotic and subsequently corresponded to high encapsulation efficiency. However, no change in NaA:SB (1:1.5) microcapsule structure was observed. The schematic diagram of Alginate-SB microcapsule structures loaded with probiotic *L. rhamnosus* is demonstrated in Fig. 2. The inner surfaces of NaA:SB (1:0) and NaA:SB (1:1.5) microcapsules (Fig. 1k and l, respectively) were similar in structure with their exterior surfaces. The probiotic was clearly observed in both microcapsules. Despite the favourable adhesion of *L. rhamnosus* on SB surface, small populations of the probiotic was seen unattached to SB and remained on the surface of alginate (Fig. 1l).

After the heat exposure was performed, the microcapsules were found to shrunk and creased in shape. Furthermore, this change was more evident on the structure of microcapsule without incorporation of SB. Both microcapsules from NaA:SB (1:0) and NaA:SB (1:1.5) loaded with probiotic (Fig. 1m and n, respectively) showed this heat effect. This is due to high dense and less porous structure of NaA:SB (1:1.5) microcapsule that reduced the penetration of heat into its structure hence *L. rhamnosus* could still be seen on the surface of the microcapsule. In contrast, the probiotic was hardly seen on the surface of NaA:SB (1:0) perhaps due to its shrunken heated structure. In addition, the porous regions of NaA:SB (1:0) surface were clearly seen after heat exposure. Meanwhile, the NaA:SB (1:1.5) microcapsule surface did not change much as it still maintained the original contour and structure. The inner surface of both microcapsules (Fig. 1o and p) obviously illustrated different observation of probiotic survavility. Fig. 1o showed very small populations of *L. rhamnosus* that can be monitored. Interestingly, the dense population of the probiotic was clearly demonstrated in Fig. 1p which reflected the heat barrier provided by the matrix of its microcapsule. Indeed, compact structure of encapsulant matrices is one of the major factors in preventing the heat penetration and its effect on the cells (Chitprasert et al., 2012). For quantitative evaluation, value of viable cell after the heat exposure was enumerated and examined in later section.

3.4. FTIR characterization

In Fig. 3, FTIR spectra referred to SB, *L. rhamnosus* NRRL 442 and immobilization of *L. rhamnosus* on SB (Immo SB + Lr). The spectra of SB and *L. rhamnosus* were analyzed first as those materials are the main components in immobilization process. SB is a lignocellulosic fibre whose major components are cellulose, hemicellulose and lignin. SB spectrum demonstrated a broad band at 3420 cm^{-1} which can be attributed to O—H stretching vibrations. The peaks appearing at 2923 and 2853 cm^{-1} belonged to the axial deformation of symmetric and asymmetric of C—H group. The peak at 1716 cm^{-1} represented the carbonyl bond (C=O) of the hemicelluloses. At 1646 cm^{-1}, the appeared absorption is related to the conjugated carbonyl bond of lignin. Symmetric deformation of CH_2 group of cellulose was indicated by bands at 1456 cm^{-1}. The band in the region of 1247 cm^{-1} was attributed to C—O—C stretching vibrations in cellulose chain. Peaks at 1106 and 1052 cm^{-1} were representative of primary and secondary hydroxide groups (C—O—C and C—O stretch).

FTIR spectra of *L. rhamnosus* showed peaks in certain areas. O—H stretching was seen at 3416 cm^{-1}. The typical functional group of fatty acids as cell membrane components was represented by asymmetric stretching vibrations of CH_3 and CH_2 which at 2923 and 2853 cm^{-1}, respectively. The broad peak at 1640 cm^{-1} and very weak peaks at 1544, 1452 and 1409 cm^{-1} were characteristic of protein content from the probiotic. The observed absorption bands at 1239 and 1061 cm^{-1} were representative of phosphodiester backbone of nucleic acid (P=O group) and components of cell wall (C—O—C group), respectively.

During the immobilization process, the interaction of SB and *L. rhamnosus* was observed as the shifting of several peaks and change of peak intensity occurred. The O-H band was shifted by −19 cm^{-1}. Peaks at 2923, 2853 and 1456 cm^{-1} exist and remained. The peak of carbonyl bond (C=O) was denoted at 1738 cm^{-1} with shifting of +22 cm^{-1}. The protein content from the probiotic was clearly

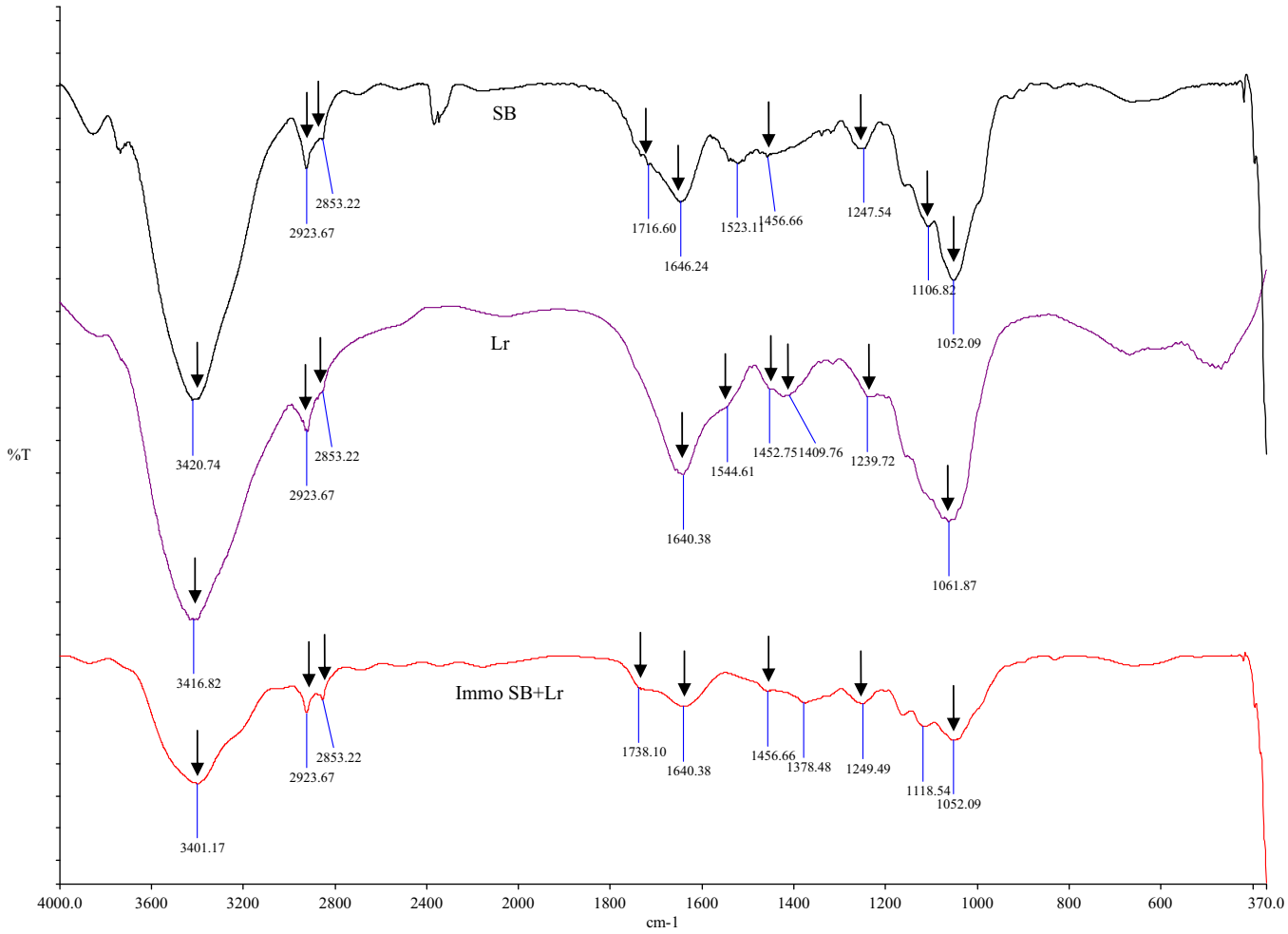

Fig. 3. FTIR spectra of SB, *L. rhamnosus* and immobilized *L. rhamnosus* on SB.

demonstrated at 1640 cm^{-1} with higher intensity. It showed that the probiotic was covering the lignin region which has the peak of 1456 cm^{-1} of SB. Presence of C═O group from the *L. rhamnosus* dense population has covered most regions of SB's surface. Meanwhile, the probiotic presence also affected the C—O—C stretching vibrations which shifted by +9 cm^{-1} to 1252 cm^{-1} which combined with the C—O—C group of SB. Most of the bands in the SB and *L. rhamnosus* spectra were still present which showed no obvious change in the functional groups of both components after the immobilization process. Peak of C—O stretching at 1052 cm^{-1} was remained.

Meanwhile, Fig. 4 showed the FTIR spectra of calcium alginate (CaA), NaA:SB (1:0) and NaA:SB (1:1.5). CaA was the main component in microencapsulation process and performed as encapsulant agent. In CaA spectra, the observed large absorption at 3432 cm^{-1} represented the deformation of O—H group. The appeared band at 1634 cm^{-1} referred to asymmetric COO^- group, while those of symmetric COO^- group was denoted at 1431 cm^{-1}. At 1081 cm^{-1}, the appeared absorption is related to the asymmetric of carbonyl bond (C—O).

The FTIR result demonstrated the interaction between the *L. rhamnosus*, immobilized *L. rhamnosus* on SB and CaA during the formation of cell-loaded microcapsule. First, this was evidenced in the encapsulated microcapsule loaded with *L. rhamnosus* (ME CaA + Lr) by shifting of O—H stretching by +16 with higher intensity band. This was due to the presence of CaA during the microencapsulation process with the occurrence of more intermolecular hydrogen bonding occurred. The asymmetric stretching vibrations of CH_3 and CH_2 of *L. rhamnosus* located at 2923 and 2853 cm^{-1} were still present. Again, the presence of CaA as encapsulant agent had covered the surface area of microcapsule and contributed to the appearance of new peaks at 1634 and 1431 cm^{-1} which were attributed to asymmetric and symmetric of COO^- group of CaA, respectively. This situation confirmed the formation of CaA matrices as encapsulant agent. Meanwhile, the protein represented by peaks of *L. rhamnosus* at 1640, 1544, 1452 and 1409 cm^{-1} disappeared. Similar situation was seen at the peak of P═O group as the CaA was the dominant component on the microcapsule surface. The peak at 1061 cm^{-1} which was denoted to the cell wall of *L. rhamnosus* still existed.

In the case of microcapsule loaded with immobilized *L. rhamnosus* on SB (ME CaA immo SB + Lr, the FTIR spectra demonstrated similar bands which were present in the spectrum of the encapsulated microcapsule loaded with *L. rhamnosus* (ME CaA + Lr). The ME CaA + Lr microcapsule spectrum was referred as control in this comparison. The broad band was observed at 1640 cm^{-1} with increased intensity which can be attributed to the increase number of *L. rhamnosus* presence on surface. This was corroborated with the observation of clear rod-shaped probiotic on the surface of the microcapsule of immobilized *L. rhamnosus* NRRL 442. The increased intensity of the band was believed to be closely related with high microencapsulation efficiency.

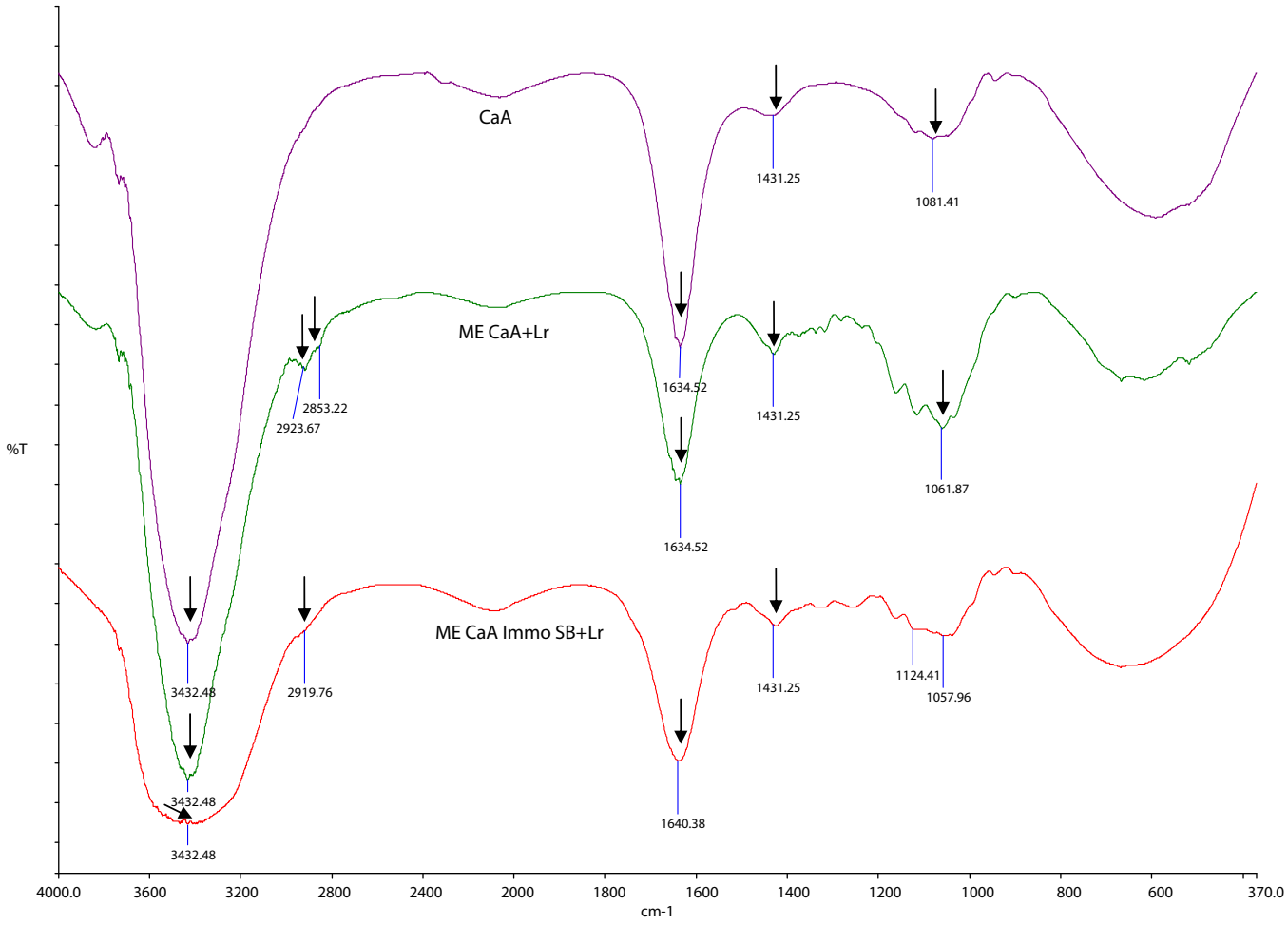

Fig. 4. FTIR spectra of CaA, microcapsule without *L. rhamnosus* and microcapsule loaded with *L. rhamnosus*.

3.5. Survivability of immobilized L. rhamnosus NRRL 442 and microencapsulated L. rhamnosus NRRL 442 after heat exposure

The heat condition of 90 °C for 30 s simulates the real situation of heat exposure and its effect (Amerah et al., 2013). Cell survivability percentage of immobilized *L. rhamnosus* NRRL 442 was analyzed and demonstrated in Table 3. The free cell was used as control. Immobilization of *L. rhamnosus* on SB improves the cell survivability after heat exposure compare to control. Significant values of survivability were obtained between the immobilized *L. rhamnosus* (55–56%) compared to free cell (32%). Heat exposure reduced the cell viability of immobilized *L. rhamnosus* and free cell up to 3.9 and 6.1 folds of log CFU/g, respectively. Better protection was due to varied heat intensity transferred to immobilized *L. rhamnosus* compared to free cell. Heat was disseminated to all area of SB and reduced the heat transfer to the immobilized probiotic. Flat surface was observed in the SEM image of SB in previous study (Shaharuddin et al., 2014) which enhances the heat transfer on the surface and reduced the heat intensity exposed to the probiotics. In other words, less direct heat of 90 °C was suffered by the probiotics. Previous study stated that immobilization of *Kluyveromyces marxianus* IMB3 on apple piece was suitable for high temperature-wine fermentation (Kourkoutas, Kanellaki, & Koutinas, 2006).

The cell survivability after heat exposure was investigated in order to determine the potential of encapsulant agent to protect the probiotic (microencapsulated cell). The free cell was the non-microencapsulated probiotic and referred as control. Heat protection provided by the encapsulant agent was proved by the significant difference in cell survivability between the microencapsulated and free cell (Table 4). Free cell of *L. rhamnosus* NRRL 442 was a heat sensitive probiotic as its viability reduced tremendously from 8.62 ± 0.30 log to 3.00 ± 0.19 log. Statistical analysis demonstrated the microencapsulated cell achieved higher significance results of cell survivability after heat exposure compared to free cell. The probiotic could survive up to ~4.5 log CFU/g which resulted in 81.30 ± 0.30% of cell survivability via microcapsule synthesized using 3% of NaA concentration onto the NaA:SB (1:1.5). The level of cell survivability was free cell < microencapsulated cell with non-inclusion of SB < microencapsulated cell with inclusion of SB.

Using ratio of NaA:SB (1:0), survivability of microencapsulated probiotic with 3% NaA (77.67 ± 0.54) was significantly higher compare to 1% and 2% (42.39 ± 1.54 and 61.57 ± 4.01, respectively). Higher concentration of NaA formed complex encapsulant matrices and minimized the free volume in the microcapsule, subsequently reducing the permeability of heat. Mandal et al. (2006) stated that slow diffusion of hot water led to higher survival of probiotic after heat exposure. In addition, heat transfer was reduced during heat exposure via complex layer of alginate. The reduction occurred during each transfer from layer to layer. Microcapsules synthesized using 3% of NaA produced larger diameter size compared to 1% and 2%. Fast radial mass transfer was facilitated with small size of microcapsule and it relates well the cell survival of these three different concentrations of NaA.

Table 3
Survival of *Lactobacillus rhamnosus* NRRL 442 after immobilization and heat exposure at 90 °C and 30 s.

Sample	Cell viability after immobilization [log CFU/g]	Cell viability after heat exposure [log CFU/g]	Cell survival (%)
SB	8.86 ± 0.04	4.95 ± 0.05	55.86 ± 0.56[b]
C	–	2.87 ± 0.03	32.03 ± 0.37[a]

Means with different superscripts (a and b) within a column were significantly different [$P < 0.05$, $n = 3$].

Table 4
Cell survival of free and microencapsulated *L. rhamnosus* NRRL 442 under different condition of synthesis after heat exposure at 90° for 30 s.

NaA concentration (%)	NaA:SB ratio	Initial cells (log CFU/g microcapsule)	Final cells (log CFU/g microcapsule)	Cell survivability (%)
Free cells	–	8.62 ± 0.30	3.00 ± 0.19	34.51 ± 2.15[a]
Microencapsulated cells				
	1:0	7.90 ± 0.16	3.34 ± 0.12	42.39 ± 1.54[b]
1	1:1.1	7.93 ± 0.07	5.68 ± 0.11	71.67 ± 1.44[d]
	1:1.5	8.13 ± 0.09	6.50 ± 0.17	80.02 ± 2.13[fg]
	1:0	7.93 ± 0.07	4.88 ± 0.32	61.57 ± 4.01[c]
2	1:1.1	8.13 ± 0.04	7.21 ± 0.14	76.33 ± 1.73[e]
	1:1.5	8.13 ± 0.03	6.25 ± 0.06	76.87 ± 0.75[ef]
	1:0	7.75 ± 0.08	5.94 ± 0.04	77.67 ± 0.54[ef]
3	1:1.1	7.98 ± 0.10	5.96 ± 0.11	74.78 ± 1.40[de]
	1:1.5	8.04 ± 0.08	7.49 ± 0.06	81.30 ± 0.30[g]

Means with different superscripts (a–g) within a column were significantly different [$P < 0.05$, $n = 3$].

Results revealed in Table 4 stated that higher inclusion of SB ratio in microencapsulation process obtained significantly higher cell survivability compared to free cell and microencapsulated cell with non-inclusion of SB. Interestingly, protection against the heat can be provided using as low as 1% of NaA and inclusion of SB. After the heat exposure, SEM images of Fig. 1m and o have clearly shown the porous regions and high loss of cell viability in microcapsules without incorporated SB, respectively. It was confirmed that better protection against heat as denser structure was observed in SEM image of the microcapsules incorporated with SB (Fig. 1p). The highest cell survivability was observed in the ones synthesized using 3% of NaA and NaA:SB ratio of 1:1.5 (81.30 ± 0.30%). However, the values of cell survivability for the increasing of NaA percentage (1, 2 and 3%) with 1:1.5 of NaA:SB ratio showed no significant difference (80.02 ± 2.13%, 76.87 ± 0.75% and 81.30 ± 0.30%, respectively). The effect of fast radial mass of small microcapsule was lightened with the presence of SB. For future upscaling purpose, lower usage of concentration of NaA is favourable as it will reduce the cost of encapsulant material and total production.

The inclusion of SB created higher density structure and longer diffusion path of heat penetration and distribution. This led to higher survivability of microencapsulated cell during heat exposure and this was confirmed by retained cell viability. However, effect of direct heat on the surface of microcapsules influenced loss of viable cell. Previously, there were two ways of increasing the characteristic of thermotolerance of microencapsulated cell; increase the concentration of encapsulant agent or incorporation of biomaterials with encapsulant agent. Mandal et al. (2006) and Ding and Shah (2007) reported the increasing of cell survivability after heat treatment was due to increasing of alginate concentration. Other researchers opted to use biomaterials such as gellan gum (Chen et al., 2007), corn starch (Sabikhi et al., 2010) or rice bran (Chitprasert et al., 2012). Chen et al., 2007 obtained optimum encapsulant combination using 2% of sodium alginate and 1% of gellan gum in encapsulation of *Bifidobacterium bifidum*. Meanwhile, corn starch was used as filler in calcium-alginate beads for encapsulation of *Lactobacillus acidophilus* LA1 and the cell viability reported reduced from 7.44 log to 3.40 log after heating at 90 °C for 30 s. Chitprasert et al. (2012) agreed that the inclusion of rice bran in *L. reuteri* KUB-AC5 entrapment increased the cell survivability after heat exposure of 85 °C for 25 s.

4. Conclusions

Overall, increasing the ratio of NaA:SB would significantly increase the cell survivability after microencapsulation and heat exposure. This beneficial step contributes in achieving high efficiency even with the usage as low as 1% NaA concentration. This study could be useful in the production of pelleted feed or other products that necessitate heat treatment.

Acknowledgements

The authors would like to thank the Department of Bioprocess Engineering, Faculty of Chemical Engineering, financial support from RMC Universiti Teknologi Malaysia and MyPhD Grant from Ministry of Higher Education (MOHE), Malaysia. In addition, the kindly supplied of probiotic strain (*Lactobacillus rhamnosus* NRRL 442) from Agricultural Research Service (ARS), USA was gratefully appreciated.

References

Amerah, A. M., Quiles, A., Medel, P., Sánchez, J., Lehtinen, M. J., & Gracia, M. I. (2013). Effect of pelleting temperature and probiotic supplementation on growth performance and immune function of broilers fed maize/soy-based diets. *Animal Feed Science and Technology*, *180*(1–4), 55–63.

Anal, A. K., & Singh, H. (2007). Recent advances in microencapsulation of probitocs for industrial applications and targeted delivery. *Trends in Food Science and Technology*, *18*, 240–251.

Borgogna, M., Bellich, B., Zorzin, L., Lapasin, R., & Cesaro, A. (2010). Food microencapsulation of bioactive compounds: Rheological and thermal characterisation of non-conventional gelling system. *Food Chemistry*, *122*(2), 416–423.

Bosnea, L. A., Kourkoutas, Y., Albantaki, N., Tzia, C., Koutinas, A. A., & Kanellaki, M. (2009). Functionality of freeze-dried *L. casei* cells immobilized on wheat grains. *LWT – Food Science and Technology*, *42*(10), 1696–1702.

Burgain, J., Gaiani, C., Linder, M., & Scher, J. (2011). Encapsulation of probiotic living cells: From laboratory scale to industrial applications. *Journal of Food Engineering*, *104*, 467–483.

Chen, M., Chen, K., & Kuo, Y. (2007). Optimal thermotolerance of *Bifidobacterium bifidum* in gellan – Alginate microparticles. *Biotechnology and Bioengineering*, *98*(2), 411–419.

Chitprasert, P., Sudsai, P., & Rodklongtan, A. (2012). Aluminum carboxymethyl cellulose–rice bran microcapsules: Enhancing survival of *Lactobacillus reuteri* KUB-AC5. *Carbohydrate Polymers*, *90*(1), 78–86.

Corbo, M. R., Bevilacqua, A., Gallo, M., Speranza, B., & Sinigaglia, M. (2013). Immobilization and microencapsulation of *Lactobacillus plantarum*: Performances and in vivo applications. *Innovative Food Science & Emerging Technologies*, *18*, 196–201.

De Vos, P., Faas, M. M., Spasojevic, M., & Sikkema, J. (2010). Encapsulation for preservation of functionality and targeted delivery of bioactive food components. *International Dairy Journal*, *20*(4), 292–302.

Ding, W. K., & Shah, N. P. (2007). Acid, bile, and heat tolerance of free and microencapsulated probiotic bacteria. *Journal of Food Science*, *72*(9), M446–M450.

Ding, W. K., & Shah, N. P. (2009). An improved method of microencapsulation of probiotic bacteria for their stability in acidic and bile conditions during storage. *Journal of Food Science*, *74*(2), M53–M61.

FAO/WHO. (2002). *Joint FAO/WHO (Food and Agriculture Organization/World Health Organization) Working Group Report on Drafting Guidelines for the Evaluation of Probiotics in Food. Guidelines for the Evaluation of Probiotics in Food. Joint Working Group Report on Drafting, London, Ontario*.

Gaggìa, F., Mattarelli, P., & Biavati, B. (2010). Probiotics and prebiotics in animal feeding for safe food production. *International Journal of Food Microbiology*, *141*, S15–S28.

Jagannath, A., Raju, P. S., & Bawa, A. S. (2010). Comparative evaluation of bacterial cellulose (nata) as a cryoprotectant and carrier support during the freeze drying process of probiotic lactic acid bacteria. *LWT – Food Science and Technology*, *43*(8), 1197–1203.

Kannoujia, D. K., Ali, S., & Nahar, P. (2009). Pressure-induced covalent immobilization of enzymes onto solid surface. *Biochemical Engineering Journal*, *48*(1), 136–140.

Karakuş, E., & Pekyardımcı, S. (2009). Immobilization of apricot pectinesterase (*Prunus armeniaca* L.) on porous glass beads and its characterization. *Journal of Molecular Catalysis B: Enzymatic*, *56*(1), 13–19.

Karnitz, O., Gurgel, L. V. A., & Gil, L. F. (2010). Removal of Ca(II) and Mg(II) from aqueous single metal solutions by mercerized cellulose and mercerized sugarcane bagasse grafted with EDTA dianhydride (EDTAD). *Carbohydrate Polymers*, *79*(1), 184–191.

Kosin, B., & Rakshit, S. K. (2010). Induction of heat tolerance in autochthonous and allochthonous thermotolerant probiotics for application to white shrimp feed. *Aquaculture*, *306*(1–4), 302–309.

Kourkoutas, Y., Bekatorou, A., Banat, I., Marchant, R., & Koutinas, A. (2004). Immobilization technologies and support materials suitable in alcohol beverages production: A review. *Food Microbiology*, *21*(4), 377–397.

Kourkoutas, Y., Xolias, V., Kallis, M., Bezirtzoglou, E., & Kanellaki, M. (2005). *Lactobacillus casei* cell immobilization on fruit pieces for probiotic additive, fermented milk and lactic acid production. *Process Biochemistry*, *40*, 411–416.

Kourkoutas, Y., Bosnea, L., Taboukos, S., Baras, C., Lambrou, D., & Kanellaki, M. (2006). Probiotic cheese production using *Lactobacillus casei* cells immobilized on fruit pieces. *Journal of Dairy Science*, *89*(5), 1439–1451.

Kourkoutas, Y., Kanellaki, M., & Koutinas, A. A. (2006). Apple pieces as immobilization support of various microorganisms. *LWT – Food Science and Technology*, *39*(9), 980–986.

Krasaekoopt, W., Bhandari, B., & Deeth, H. (2003). Evaluation of encapsulation techniques of probiotics for yoghurt. *International Dairy Journal*, *13*(1), 3–13.

Mandal, A., & Chakrabarty, D. (2011). Isolation of nanocellulose from waste sugarcane bagasse (SCB) and its characterization. *Carbohydrate Polymers*, *86*(3), 1291–1299.

Mandal, S., Puniya, A. K., & Singh, K. (2006). Effect of alginate concentrations on survival of microencapsulated *Lactobacillus casei* NCDC-298. *International Dairy Journal*, *16*(10), 1190–1195.

Michida, H., Tamalampudi, S., Pandiella, S. S., Webb, C., Fukuda, H., & Kondo, A. (2006). Effect of cereal extracts and cereal fiber on viability of Lactobacillus plantarum under gastrointestinal tract conditions. *Biochemical Engineering Journal*, *28*(1), 73–78.

Nagar, S., Mittal, A., Kumar, D., Kumar, L., & Gupta, V. K. (2012). Immobilization of xylanase on glutaraldehyde activated aluminum oxide pellets for increasing digestibility of poultry feed. *Process Biochemistry*, *47*(9), 1402–1410.

Noriega, E., Velliou, E., Van Derlinden, E., Mertens, L., & Van Impe, J. F. M. (2013). Effect of cell immobilization on heat-induced sublethal injury of *Escherichia coli*, *Salmonella typhimurium* and *Listeria innocua*. *Food Microbiology*, *36*(2), 355–364.

Quan, J., Liu, Z., Branford-White, C., Nie, H., & Zhu, L. (2014). Fabrication of glycopolymer/MWCNTs composite nanofibers and its enzyme immobilization applications. *Colloids and Surfaces B: Biointerfaces*, *121*, 417–424.

Reddy, L. V., Reddy, Y. H. K., Reddy, L. P. A., & Reddy, O. V. S. (2008). Wine production by novel yeast biocatalyst prepared by immobilization on watermelon (*Citrullus vulgaris*) rind pieces and characterization of volatile compounds. *Process Biochemistry*, *43*(7), 748–752.

Rokka, S., & Rantamaki, P. (2010). Protecting probiotic bacteria by microencapsulation: Challenges for industrial applications. *European Food Research and Technology*, *23*, 1–12.

Sabikhi, L., Babu, R., Thompkinson, D. K., & Kapila, S. (2010). Resistance of microencapsulated *Lactobacillus acidophilus* LA1 to processing treatments and simulated gut conditions. *Food and Bioprocess Technology*, *3*(4), 586–593.

Seo, J. K., Kim, S. W., Kim, M. H., Upadhaya, S. D., Kam, D. K., & Ha, J. K. (2010). Direct-fed microbials for ruminant animals. *Asian-Australasian Journal of Animal Sciences*, *23*(12), 1657–1667.

Seng, K. F., Muhamad, I. I., Tin, L. C., Razali, F., Pae, N., & Shaharudin, S. (2012). Effect of pH and temperature on the growth and B-glucosidase activity of Lactobacillus rhamnosus NRRL 442 in anaerobic fermentation. *International Review of Chemical Engineering*, *4*(3), 293–299.

Shaharuddin, S., Muhamad, I. I., Seng, K. F., Zahan, K. A., & Khairuddin, N. (2014). Potential use of biofibers for functional immobilization of *Lactobacillus rhamnosus* NRRL 442. *Key Engineering Materials*, *595*, 231–235.

Vercelheze, A. E. S., Fakhouri, F. M., Dall'Antônia, L. H., Urbano, A., Youssef, E. Y., Yamashita, F., et al. (2012). Properties of baked foams based on cassava starch, sugarcane bagasse fibers and montmorillonite. *Carbohydrate Polymers*, *87*(2), 1302–1310.